

# Magneto-optical trapping and ultracold collisions of potassium atoms

R. S. Williamson III and T. Walker

*Department of Physics, University of Wisconsin—Madison, Madison, Wisconsin 53706*

Received September 29, 1994; revised manuscript received March 22, 1995

We present measurements of loading and loss rates for a vapor-cell optical trap of the two naturally occurring potassium isotopes  $^{39}\text{K}$  and  $^{41}\text{K}$ . The unresolved excited-state hyperfine structure makes trapping of K fundamentally different from trapping of the other alkalis and leads to an enhanced loading rate. We measure the loading rate as a function of laser intensity, beam size, and detuning and find that the results are in reasonable agreement with a simple rate-equation model for the loading process. The dependence of the loss rate on trapped-atom density determines the contribution to the loss rates from excited-state collisions. We find a substantial difference between the collisional loss rates for the two isotopes.

## 1. INTRODUCTION

To date, a variety of atoms have been stably cooled and confined by use of magneto-optical traps (MOT's). Since the original demonstration with Na,<sup>1</sup> MOT's have been constructed for the alkalis Li,<sup>2</sup> Rb,<sup>3</sup> and Cs,<sup>4</sup> the alkaline-earth atoms Mg,<sup>5</sup> Ca,<sup>6</sup> and Sr,<sup>6</sup> and the metastable states of the rare gases He,<sup>7</sup> Ne,<sup>8</sup> Ar,<sup>9</sup> Kr,<sup>9</sup> and Xe.<sup>10</sup> All these atoms are characterized by their relatively simple energy-level structures, so that trapping can be accomplished by use of a small number of laser frequencies. In addition, the wavelengths for the trapping transitions are all in the near ultraviolet to near infrared, for which tunable continuous-wave lasers exist with powers exceeding 1 mW.

Notably absent from the above list is the alkali atom K, which has a convenient resonance line at 767 nm. K is unique among the alkalis in that the nuclear magnetic moments of its isotopes are comparatively quite small, leading to correspondingly small hyperfine splittings of the optical transitions. As explained below, this necessitates a different approach to making a MOT for K. Although Li also has small excited-state hyperfine splittings, the structure is inverted compared with the other alkalis, so one still does the trapping by tuning near the  $S_{1/2}(F = I + 1/2) \rightarrow P_{3/2}(F' = I + 3/2)$  transition, as is done for Na, Rb, and Cs.

In this paper we present a two-part study of the basic properties of a K MOT. In Section 2 we describe measurements relating to the performance of the trap itself, including loading rates and loss rates, and in Section 3 we focus on measurements of the loss rates that are due to ultracold collisions.

## 2. MAGNETO-OPTICAL TRAPPING OF K

In this section we present our observations of the K MOT. The relevant energy levels for the common isotopes of K are shown in Fig. 1. Note that, even for  $^{39}\text{K}$ , which has the larger hyperfine interaction, the splitting between the  $P_{3/2}(F' = 3)$  and  $(F' = 2)$  states is only 21 MHz, com-

pared with the natural linewidth of 6.2 MHz. If the trapping laser frequency is chosen to be near the  $4S_{1/2}(F = 2) \rightarrow 4P_{3/2}(F' = 3)$  transition (the analogous transition for other alkali MOT's), there will be strong heating and optical pumping of the atoms into the  $4S_{1/2}(F = 1)$  state as a result of the nearby  $4P_{3/2}(F' = 2)$  state, thus preventing trapping. In addition, power broadening will reduce the spectral isolation needed for trapping in the usual manner.

To avoid these problems, we trap K by using light tuned to the low-frequency side of the entire excited-state hyperfine structure, as shown in Fig. 1. Two laser frequencies are used, differing by the ground-state hyperfine splitting. Both frequencies provide cooling and trapping forces. This arrangement has the advantage over other MOT's that the poorly resolved excited-state hyperfine structure creates an intrinsically large capture velocity for the trap. We illustrate this in Fig. 2, which shows the calculated light-induced damping force as a function of frequency. The force is substantial over a region of 35 MHz, corresponding to an intrinsic capture velocity for the trap exceeding 30 m/s.

As an aside, we note that  $P_{1/2}$  states of K have significantly larger hyperfine interactions than the  $P_{3/2}$  states, so the levels are well resolved. Simple models of the MOT trapping force suggest that trapping with light tuned to the  $P_{1/2}$  states should be possible. However, we have not been able to trap either isotope of K using the  $P_{1/2}$  states. We see no fundamental reasons why the  $P_{1/2}$  states cannot be used for trapping in a manner analogous to the  $P_{3/2}$  type II trap originally demonstrated with Na (Ref. 1); thus a more detailed analysis is needed to explain this observation.<sup>14</sup>

A simplified schematic of our apparatus appears in Fig. 3. The laser light is provided by an Ar-ion-pumped Ti:sapphire laser, purged with dry  $\text{N}_2$  to eliminate the destabilizing effects of  $\text{O}_2$ , which has an absorption feature near 766.7 nm. Using an acousto-optic modulator, we stabilize the laser to the  $S_{1/2}(F = 2) \rightarrow P_{3/2}$  transition by offset locking to the  $^{39}\text{K}$   $S_{1/2}(F = 2) \rightarrow P_{3/2}$  saturation spectroscopy peak. Because the excited-state hyperfine

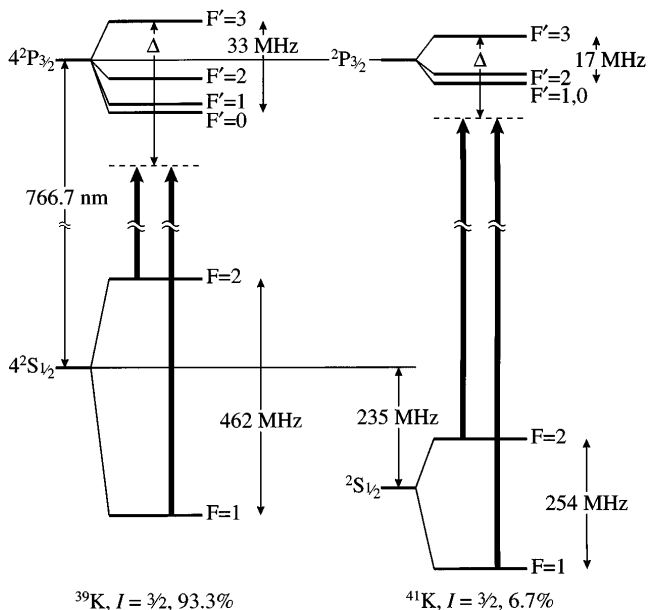


Fig. 1. Hyperfine structure of the  $4^2S_{1/2}$  and  $4^2P_{3/2}$  states of the two abundant isotopes of K. The thick vertical lines indicate the two laser frequencies. Note that the detuning  $\Delta$  is measured from the  $4^2S_{1/2}(F = 2)$  or  $4^2P_{3/2}(F' = 3)$  transition. For reference, the hyperfine constants for the various states are  $^{39}\text{K}$ ,  $A(S_{1/2}) = 230.9$  MHz,  $A(P_{3/2}) = 6.1$  MHz,  $B(P_{3/2}) = 2.8$  MHz;  $^{41}\text{K}$ ,  $A(S_{1/2}) = 127.0$  MHz,  $A(P_{3/2}) = 3.4$  MHz,  $B(P_{3/2}) = 3.3$  MHz.<sup>11</sup> The isotope shift is 235.3 MHz,<sup>12</sup> and the excited-state lifetime is 25.8 ns.<sup>13</sup>

structure is unresolved, this leads to a 2–3-MHz uncertainty in the detuning  $\Delta$ . Part of the light is sent to a second acousto-optic modulator whose frequency is fixed to the ground-state hyperfine splitting, providing the necessary  $S_{1/2}(F = 1) \rightarrow P_{3/2}$  light. The output beam from the acousto-optic modulator and the unmodulated beam are adjusted for equal power and then combined and sent through the trapping chamber. Right-angle prisms, with axes mounted orthogonally to minimize effects of diffraction from their apices, are used to retroreflect the large beams. With this precaution the use of prisms rather than wave plates and mirrors does not significantly degrade the operation of the trap (the number of atoms is

reduced by only  $\sim 20\%$ ). This simplifies the apparatus by eliminating the need for a large mirror and wave plate for each beam.

The trapping chamber is a stainless-steel ion-pumped vacuum system containing room-temperature K vapor at a pressure of  $3 \times 10^{-9}$  Torr (K density,  $1 \times 10^8$  cm $^{-3}$ ). Magnetic-field gradient and shim coils are wrapped around the outside of the chamber; the shim coils are necessary to counteract the intensity imbalance induced by the uncoated windows of the chamber and the retroreflecting prisms. A photodetector measures the fluorescence of the atoms as they are loaded from the vapor, and a video camera is used to determine the size of the trapped-atom cloud. From these measurements we also deduce the density.

The remainder of this paper will focus on loading and loss rates deduced by measurement of the number of atoms as a function of time as the atoms load into an empty trap:

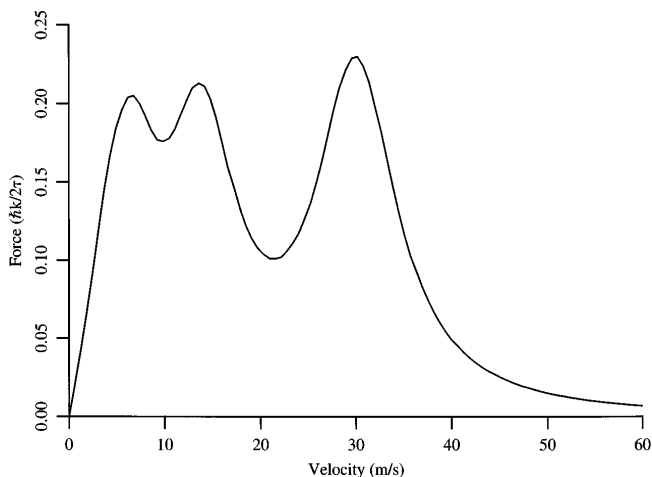


Fig. 2. Plot showing that light exerts force on a moving K atom over a wide velocity range, illustrating how the small excited-state hyperfine structure produces a large capture velocity. This is the result of running our model for  $^{39}\text{K}$  with a laser intensity of 270 mW/cm $^2$  and a detuning  $\Delta = -39$  MHz.

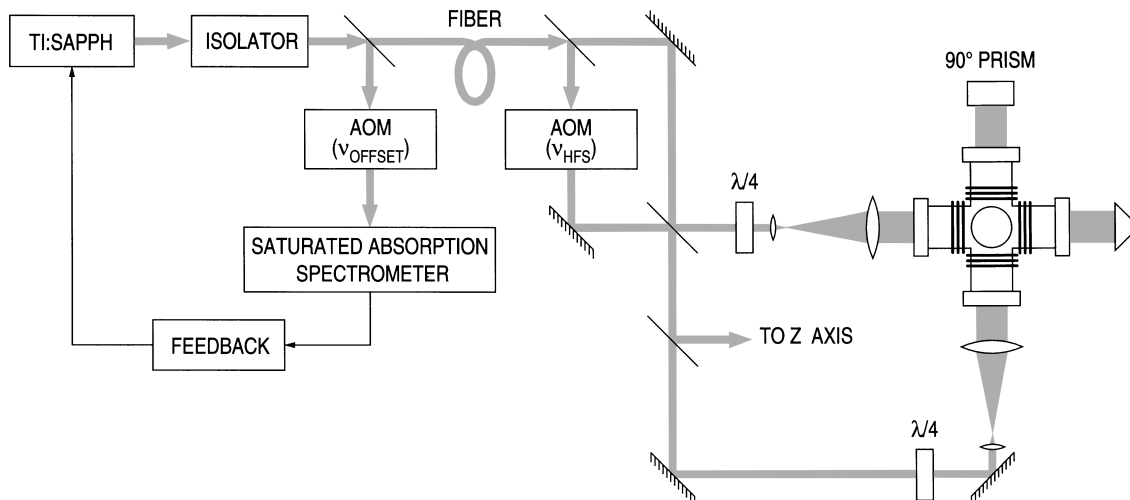


Fig. 3. Simple schematic of the trapping apparatus. AOM's, acousto-optic modulators;  $\lambda/4$ 's, quarter-wave plates.

$$\frac{dN(t)}{dt} = l[A] - \Gamma N. \quad (1)$$

Here  $N(t)$  is the number of trapped atoms as a function of time  $t$ ,  $l$  is the loading rate coefficient (in units of cubic centimeters per second),  $[A]$  is the number density of the isotropic species being trapped, and  $\Gamma$  is the total loss rate of atoms from the trap.

Since we use the fluorescence measurements to deduce  $N$  and to understand how it varies as a function of the various parameters of the trap, it is necessary to calculate the fraction of atoms that are in excited states and the velocity-dependent force on the atoms. We have constructed a fairly simple rate-equation model for this purpose, and it seems to give reasonable results under most of the conditions that we have studied. Except for the unique characteristics of K discussed below, our model is similar to both that of Lindquist *et al.*,<sup>15</sup> who also used a rate-equation model to predict loading characteristics of a Cs-vapor-loaded MOT, and to that of Gibble *et al.*<sup>16</sup>

For K, it is essential to include the hyperfine structure in such calculations since optical pumping is extremely important. We therefore consider a six-level model (two ground states and four excited states), permitting the populations of each hyperfine state to vary, assuming uniform distributions of populations among the Zeeman sublevels of each hyperfine state. In addition, we ignore optical coherences and simply make a rate-equation model for the populations in the various states. Thus the stimulated emission and absorption rates are calculated by use of sublevel-averaged oscillator strengths, and the population in each hyperfine state is calculated by simple equalization of the excitation and emission rates. We use a saturation intensity  $I_{\text{sat}} = 3.6 \text{ mW/cm}^2$ , based on the same definition as that of Lindquist *et al.*

To calculate forces, we allow for Doppler shifts of the resonance frequencies. Since the trapping lasers come from six directions there is a different Doppler shift for each direction, but for simplicity we have constrained the atoms to have velocity along only one direction, so that only two of the beams have Doppler shifts. We obtain the force by keeping track of the scattering rates out of each of the two counterpropagating beams along the direction of motion of the atoms. The difference between the rates gives the force. A number of assumptions are inherent in this approach; in particular, we can ignore velocity-dependent dipole forces that may be quite large at high intensity. Since Lindquist *et al.* found little effect of the magnetic field on the loading rates we have similarly not included magnetic-field effects in our model.

To predict loading rates, we use the calculated forces to find the stopping distance required as a function of velocity. At low intensity the stopping distance can be interpreted as the diameter of the laser beams, but at high intensities a Gaussian beam still exerts considerable force beyond its waist  $w = d/2$ , defined as the point at which the beam intensity drops by  $1/e^2$ . For high-intensity beams, as were used in Figs. 4(b) (<sup>41</sup>K) and 5(b), we use an effective waist that occurs farther outside the beam profile, determined from the point at which the excited-state fraction corresponding to that intensity is reduced by  $1/e^2$  of the excited-state fraction at the peak of the beam. Given the capture velocity, we use

the equations of Monroe *et al.* to predict the loading rate coefficient.<sup>17</sup>

We have characterized the operation of both the <sup>39</sup>K and <sup>41</sup>K MOT's as a function of the detuning  $\Delta$ , beam diameter  $d$ , and intensity  $I_{\text{tot}}$ . Here  $I_{\text{tot}}$  refers to the sum of the laser intensities from each of the six beams and both laser frequencies. In Fig. 4 we show how the number of atoms, the loading rate coefficient, the density, and the loss rate depend on  $\Delta$ . The <sup>39</sup>K data, represented by the filled symbols, were taken at  $I_{\text{tot}} = 220 \text{ mW/cm}^2$  and  $d = 1.2 \text{ cm}$ ; the <sup>41</sup>K data, represented by open symbols, were taken at  $I_{\text{tot}} = 470 \text{ mW/cm}^2$  and  $d = 0.6 \text{ cm}$ . Both data sets were taken with a magnetic-field gradient of  $16 \text{ G/cm}$ , while the bias field was adjusted slightly (less than  $1 \text{ G}$ ) each time  $\Delta$  was changed to keep the trap centered in the beams. The magnetic-field gradient could be changed by an amount of the order of 50% without materially affecting trap operation.

Although the <sup>39</sup>K and <sup>41</sup>K data were taken under different trapping conditions, we can still compare them qualitatively. When we scale the number of atoms by the isotopic ratio, we get similar results for both. The differences in the loading rate coefficients and in density are likely due to the fact that the <sup>41</sup>K trap used smaller, more

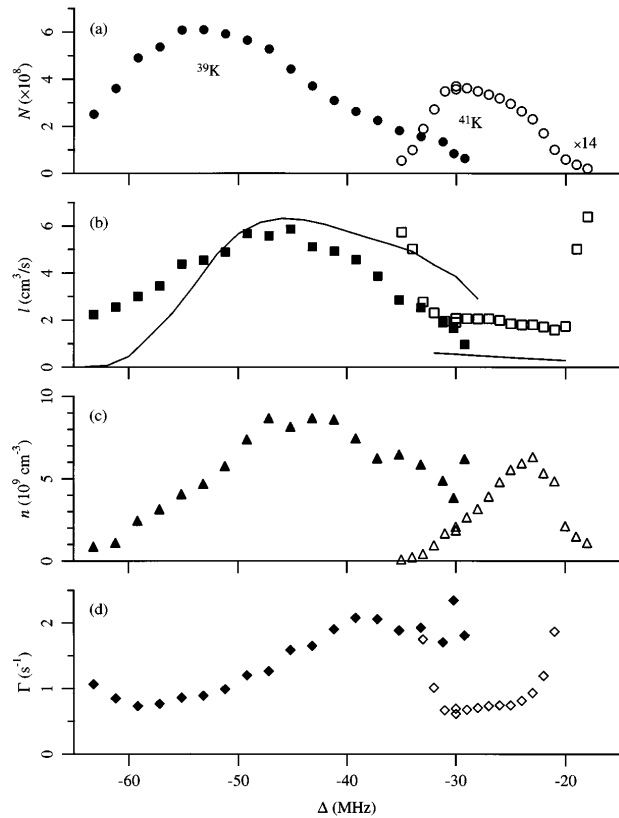


Fig. 4. (a) Number of trapped atoms  $N$ , (b) loading rate coefficient  $l$ , (c) trapped atom density  $n$ , and (d) loss rate  $\Gamma$  as functions of the trap laser detuning  $\Delta$ . The filled symbols represent <sup>39</sup>K, and the open symbols represent <sup>41</sup>K. The <sup>39</sup>K data were taken with  $I_{\text{tot}} = 220 \text{ mW/cm}^2$ ,  $d = 1.2 \text{ cm}$ , and the <sup>41</sup>K data were taken with  $I_{\text{tot}} = 470 \text{ mW/cm}^2$ ,  $d = 0.6 \text{ cm}$ . The <sup>41</sup>K data in (a) have been scaled by 13.9, the isotopic abundance ratio. The solid curves in (b) are the results of our simple loading rate model, scaled by a factor of 1.5. The operation of the trap was marginal at the ends of the detuning ranges, yielding large uncertainties in  $\Gamma$ .

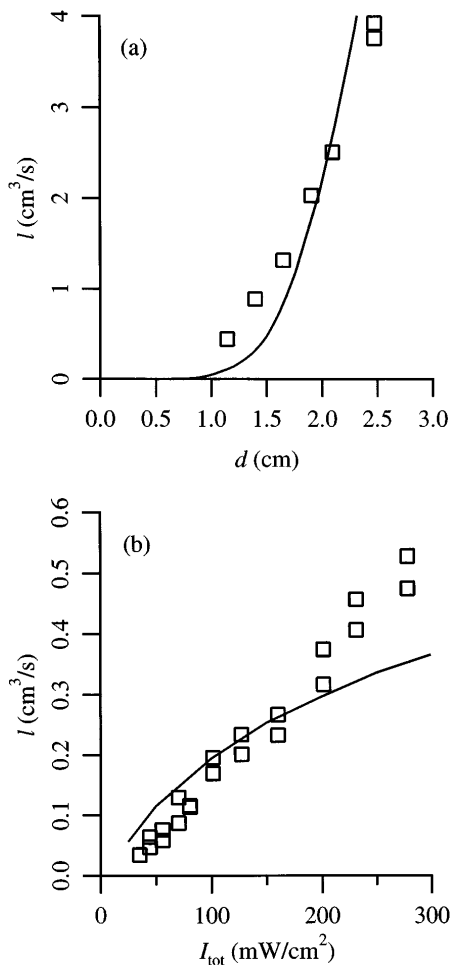


Fig. 5. Loading rate coefficient  $l$  as a function of (a) beam diameter  $d$  and of (b) intensity  $I_{\text{tot}}$  for a magnetic-field gradient of 16 G/cm, using  $^{41}\text{K}$ . In (a),  $I_{\text{tot}} = 20 \text{ mW/cm}^2$  and  $\Delta = -32 \text{ MHz}$ ; in (b),  $d = 0.6 \text{ cm}$  and  $\Delta = -21 \text{ MHz}$ . The simple loading-rate-model results (solid curves) in both cases have been scaled by a factor of 1.5.

intense beams. The difference in the loss rates between the two isotopes will be discussed in the next section.

We have also measured  $l$  as a function of  $d$  and  $I_{\text{tot}}$ , shown in Fig. 5. The model results, which have been scaled by a factor of 1.5 to give a good fit to Fig. 5(a), follow the data rather well as  $d$  is changed [Fig. 5(a)] but diverge at high  $I_{\text{tot}}$  [Fig. 5(b)]. This may be attributable to the neglect of dipole forces; nevertheless, the simple model is useful and has predictive power in the regime in which traps are normally operated. In addition, we have plotted the model results as a function of  $\Delta$  in Fig. 4(b), in which they have been scaled as before. Over a wide range of parameters, it is seen that the model is good to within a factor of 3. We note that the unscaled Lindquist *et al.* model for a Cs MOT also predicted smaller numbers of atoms than were observed. To illustrate the ability of the model to predict trends, they scaled their results by a factor of 3.3.

The trap temperature was estimated by use of a release and recapture technique<sup>18</sup> in which a fully loaded trap is turned off by having the gradient magnetic field turned off and the laser light detuned far away from resonance for a few milliseconds and is then returned to normal trap-

ping conditions (gradient on, laser tuned near resonance). By varying the amount of time the trap is off and measuring how many atoms are lost while the trap is off we can estimate the temperature of the trapped atoms. For our  $^{41}\text{K}$  MOT, with  $I_{\text{tot}} = 530 \text{ mW/cm}^2$ ,  $d = 0.6 \text{ cm}$ , and  $\Delta = -21 \text{ MHz}$ , we deduce a temperature of approximately  $200 \mu\text{K}$ .

### 3. ULTRACOLD COLLISIONS

To date, a number of studies have been made of excited-state collisions of atoms in MOT's.<sup>19</sup> These collisions are of interest because of the sensitivity of the collision dynamics to weak long-range interactions, the similarity of collision and spontaneous emission times, and the capabilities of precision molecular spectroscopy approach a few wave numbers of the dissociation limit. All these features should in principle be present in ultracold collisions of K atoms. In this section we focus on measurements of the collision rates for both abundant isotopes of K as induced by the trapping lasers.

As explained above, we determine the loss rate  $\Gamma = \gamma + \beta n$  directly from loading transients. Two processes are known to contribute to these rates. First, collisions with hot background atoms (mostly K atoms in this experiment) can eject the atoms from the trap at a rate  $\gamma$ . This process is weakly dependent on the trap depth, and therefore  $\gamma$  is likely to be insensitive to the detuning of the lasers from resonance. Second, excited-state collisions between the trapped atoms can also result in loss of atoms from the trap, with rate  $\beta n$ . The loss rate owing to this process should display a strong frequency dependence since the rate depends both on density  $n$  as well as on the collisional rate coefficient  $\beta$ . The frequency dependence of  $\beta$  arises from a number of effects, the most important of which are spontaneous emission during the collisions and modification of the dynamics by hyperfine interactions.<sup>20</sup> Figure 4(d) shows the dependence of the loss rate on detuning of  $^{39}\text{K}$ . This strongly frequency-dependent rate suggests that ultracold collisions are important in the trap.

To extract the ultracold collision rates from the data, we fix  $\Delta$  and study the dependence of the loss rates on  $n$ ,

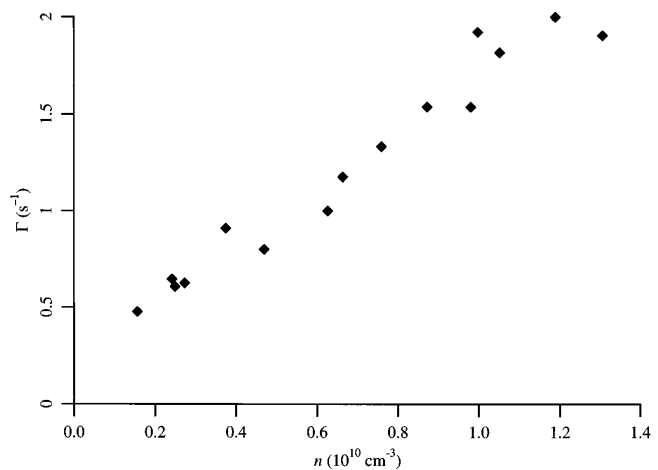


Fig. 6. Dependence of the collision rate  $\Gamma$  on the density  $n$  for  $^{39}\text{K}$  at a fixed detuning  $\Delta = -39 \text{ MHz}$  and an intensity  $I_{\text{tot}} = 250 \text{ mW/cm}^2$ .

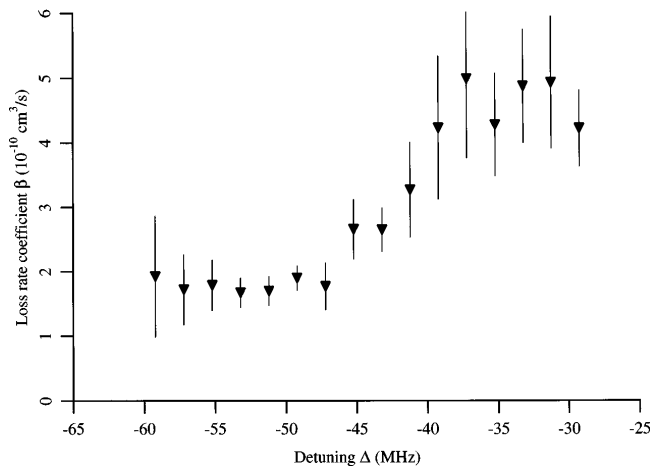


Fig. 7. Dependence of the collisional rate coefficient  $\beta$  as a function of the detuning  $\Delta$  for  $^{39}\text{K}$  at an intensity  $I_{\text{tot}} = 220 \text{ mW/cm}^2$ .

which we vary by changing the magnetic-field gradient. Typical data are shown in Fig. 6. The slope of the data gives the collisional rate coefficient  $\beta$ . Furthermore, we find that the intercept varies only slightly with  $\Delta$ , consistent with the interpretation that the intercept is due to collisions with untrapped room-temperature K atoms. We find that  $\gamma \approx 0.3 \text{ s}^{-1}$ .

Figure 7 shows the dependence of  $\beta$  on  $\Delta$ . We find little variation of  $\beta$  over the detuning range studied. This is not too surprising since the range is quite limited compared with catalysis laser experiments in which the detuning is varied by as much as 1 GHz. The absolute rates that we measure are comparable with results for the other alkalis.<sup>17</sup> Thus the detuning dependence of the loss rate shown in Fig. 4(d) arises mostly from the variation of  $n$  with  $\Delta$ . The error bars in Fig. 7 reflect observed fluctuations in measurements of  $n$  and  $\Gamma$ ; however, there may be systematics that change the axis scale.

For  $^{41}\text{K}$  the situation is quite different. Even at high intensities, we find only a slight dependence of the loss rates on detuning, except under extreme conditions of detuning and (small) magnetic-field gradients, in which the operation of the trap is marginal. We find no density-dependent effect at the level of our sensitivity, which gives an upper limit on  $\beta$  for  $^{41}\text{K}$  of  $\beta < 9 \times 10^{-11} \text{ cm}^3/\text{s}$  at  $220 \text{ mW/cm}^2$ , a factor of 3 to 5 lower than for  $^{39}\text{K}$ . Of course, these results are not directly comparable because of the different hyperfine structures and detunings. We also note that large isotope effects have been observed for Rb (Ref. 17) and in the radiative emission rates for Li.<sup>21</sup>

The principal uncertainty in the ultracold collision rates is the determination of  $n$ . Here the principal issues are the difficulty in determining the precise density distribution owing to the often asymmetrical shapes of the atom clouds and the uncertainty in the excited-state fraction. We estimate an overall uncertainty for the above results of approximately a factor of 2, based on the reproducibility of the measurements for different-shaped clouds and the different excited-state fraction.

## 4. CONCLUSIONS

We have emphasized in this paper the different issues involved in studying K atoms in a MOT. With the exception of the roles of the poorly resolved excited-state hyperfine structure, we find that the trap behaves in most respects quite similarly to the other alkalis. We have observed a striking difference in the ultracold collision rates for the two isotopes that we have trapped.

## ACKNOWLEDGMENTS

This study was supported by the National Institute for Standards and Technology, the National Science Foundation, and the Packard Foundation.

## REFERENCES AND NOTES

1. E. Raab, M. Prentiss, A. Cable, S. Chu, and D. Pritchard, *Phys. Rev. Lett.* **59**, 2631 (1987).
2. Z. Lin, K. Shimizu, M. Zhan, F. Shimizu, and H. Takuma, *Jpn. J. Appl. Phys.* **30**, L1324 (1991).
3. T. Walker, D. Hoffmann, P. Feng, and R. S. Williamson III, *Phys. Lett. A* **163**, 309 (1992).
4. D. Sesko, T. Walker, C. Monroe, A. Gallagher, and C. Wieman, *Phys. Rev. Lett.* **63**, 961 (1989).
5. K. Sengstock, U. Sterr, G. Hennig, D. Bettermann, J. H. Müller, and W. Ertmer, *Opt. Commun.* **103**, 73 (1993).
6. T. Kurosu and F. Shimizu, *Jpn. J. Appl. Phys.* **29**, L2127 (1990).
7. F. Bardou, O. Emile, J. Courty, C. Westbrook, and A. Aspect, *Europhys. Lett.* **20**, 681 (1992).
8. F. Shimizu, K. Shimizu, and H. Takuma, *Phys. Rev. A* **39**, 2758 (1989).
9. H. Katori and F. Shimizu, *Jpn. J. Appl. Phys.* **29**, L2124 (1990).
10. M. Walhout, H. J. L. Megens, A. Witte, and S. L. Rolston, *Phys. Rev. A* **48**, R879 (1993).
11. E. Arimondo, M. Inguscio, and P. Violino, *Rev. Mod. Phys.* **49**, 31 (1977).
12. N. Bendali, H. T. Duong, and J. L. Vialle, *J. Phys. B* **14**, 4231 (1981).
13. W. L. Wiese and G. A. Martin, *Wavelengths and Transition Probabilities for Atoms and Atomic Ions, Part II, Transition Probabilities*, Natl. Stand. Ref. Data Series Natl. Bur. Stand. **68**, 394 (1980).
14. P. van der Straten [Debye Institute, Utrecht University, Utrecht 3508 TA, The Netherlands (personal communication, 1994)] has confirmed, using a more sophisticated MOT simulation, that  $P_{1/2}$  trapping is extremely weak. The reason for this is not yet known.
15. K. Lindquist, M. Stephens, and C. Wieman, *Phys. Rev. A* **46**, 4082 (1992).
16. K. E. Gibble, S. Kasapi, and S. Chu, *Opt. Lett.* **17**, 526 (1992).
17. C. Monroe, W. Swann, H. Robinson, and C. Wieman, *Phys. Rev. Lett.* **65**, 1571 (1990).
18. P. D. Lett, W. D. Phillips, S. L. Rolston, C. E. Tanner, R. N. Watts, and C. I. Westbrook, *J. Opt. Soc. Am. B* **6**, 2084 (1989).
19. T. Walker and P. Feng, *Adv. At. Mol. Opt. Phys.* **34**, 125 (1994).
20. T. Walker and D. Pritchard, *Laser Phys.* **4**, 1085 (1994).
21. N. W. M. Ritchie, E. R. I. Abraham, and R. G. Hulet, *Laser Phys.* **4**, 1066 (1994).